

37p.

NASA TECHNICAL
MEMORANDUM

N64-18164 *

CODE-1

(NASA TM X-53003)

September 24, 1963

OTS.

NASA TM X-53003

**PROPOSED SOLUTION TO THE
GEOMAGNETIC ANOMALIES IN
THE IONOSPHERE**

by WILLIAM T. ROBERTS *Washington, NASA,*
Aero-Astroynamics Laboratory *24 Sep. 1963 37p*

George C. Marshall
Space Flight Center,
Huntsville, Alabama

OTS PRICE

XEROX

MICROFILM

NASA-GEORGE C. MARSHALL SPACE FLIGHT CENTER

TECHNICAL MEMORANDUM X-53003

PROPOSED SOLUTION TO THE GEOMAGNETIC
ANOMALIES IN THE IONOSPHERE

by

WILLIAM T. ROBERTS

ABSTRACT

A

18164

In order to determine the driving and controlling mechanisms which predominate in the ionosphere, a series of contour maps were drawn from IGY data taken at stations lying approximately along the seventy-fifth meridian. An attempt was then made to interpret the anomalous behavior of the F₂ peak of the ionosphere in the vicinity of the geomagnetic equator. If one assumes the existence of an equatorial electrojet and further assumes that the magnetic field which is associated with this electrojet is sufficient to perturb the earth's main magnetic field, electrons may be deflected away from the geomagnetic equator. Furthermore, if the atmosphere tends to expand and contract diurnally, ions and electrons may be deflected into regions at times which could account for the nocturnal increase in electron density north and south of the geomagnetic equator. Special emphasis is placed upon this nocturnal increase in electron density, and when its seasonal variation is investigated one finds that the phenomenon is greatest during and around the months of equinox and least so during and around the months of solstice.

Author

NASA-GEORGE C. MARSHALL SPACE FLIGHT CENTER

TECHNICAL MEMORANDUM X-53003

September 24, 1963

PROPOSED SOLUTION TO THE GEOMAGNETIC
ANOMALIES IN THE IONOSPHERE

By

William T. Roberts

SPACE ENVIRONMENT GROUP
AERO-ASTROPHYSICS OFFICE
AERO-ASTRODYNAMICS LABORATORY

ACKNOWLEDGEMENT

The author wishes to acknowledge the assistance of Mr. R. E. Smith, Chief, Space Environment Group, Aero-Astrophysics Office, Aero-Astrodynamic Laboratory, and Dr. W. Heybey of the Aero-Astrodynamic Laboratory's Technical Staff in reviewing this report, and for the many helpful technical suggestions they have contributed.

TABLE OF CONTENTS

	<u>Page</u>
SECTION I. INTRODUCTION.....	2
SECTION II. THE IONOSPHERE IN THEORY.....	2
SECTION III. DISCUSSION OF PROBLEM.....	4
SECTION IV. ELECTRONS IN A MAGNETIC FIELD.....	6
SECTION V. PRESENTATION OF THEORY.....	8
SECTION VI. LIMITATIONS OF THEORY.....	11

LIST OF ILLUSTRATIONS

<u>Figure</u>	<u>Title</u>	<u>Page</u>
1	Contours of Constant Frequency (Mc/sec) for the Peak of the F ₂ Layer Averaged Over the Month of March 1958...	13
2	Contours of Constant Frequency (Mc/sec) for the Peak of the F ₂ Layer Averaged Over the Month of July 1958....	14
3	Contours of Constant Frequency (Mc/sec) for the Peak of the F ₂ Layer Averaged Over the Month of September 1958.....	15
4	Contours of Constant Frequency (Mc/sec) for the Peak of the F ₂ Layer Averaged Over the Month of December 1958...	16
5	Contours of Constant Height (km) of the Peak of the F ₂ Layer Averaged Over the Month of March 1958.....	17
6	Contours of Constant Height (km) of the Peak of the F ₂ Layer Averaged Over the Month of July 1958.....	18
7	Contours of Constant Height (km) of the Peak of the F ₂ Layer Averaged Over the Month of September 1958.....	19
8	Contours of Constant Height (km) of the Peak of the F ₂ Layer Averaged Over the Month of December 1958.....	20
9	Contours of Constant Electron Density in Electrons per Cubic Centimeter Depicting the Height and Latitudinal Location of the Nocturnal Maximum Electron Density at 19:00 LST on March 21, 1958.....	21
10	Contours of Constant Electron Density in Electrons per Cubic Centimeter Depicting the Height and Latitudinal Location of the Nocturnal Maximum Electron Density at 19:00 LST on July 15, 1958.....	22
11	Contours of Constant Electron Density in Electrons per Cubic Centimeter Depicting the Height and Latitudinal Location of the Nocturnal Maximum Electron Density at 19:00 LST on September 22, 1958.....	23
12	Contours of Constant Electron Density in Electrons per Cubic Centimeter Depicting the Height and Latitudinal Location of the Nocturnal Maximum Electron Density at 20:00 LST on December 21, 1958.....	24

LIST OF TABLES

<u>Table</u>	<u>Title</u>	<u>Page</u>
I	Stations Used in the Construction of Figures 1-8.....	12
II	Stations Used in the Construction of Figures 9-12.....	12

DEFINITION OF SYMBOLS

<u>Symbol</u>	<u>Definition</u>
N	Electron density in electrons per cm^3
ϵ_0	Permittivity of free space
e	Charge on an electron
m	Mass of a particle
ω	Angular frequency of wave incident upon the ionosphere
f	Plasma resonance frequency
I	Spectral intensity of radiation incident at a certain height in the ionosphere
σ	Coefficient of absorption for spectral irradiation
ρ	Density of the atmosphere
χ	Zenith angle of the sun
Z	Height above the earth's surface
F_2	The region in the ionosphere which contains the highest electron concentration
f_0F_2	The "critical frequency" of the ionosphere, where any higher frequency will penetrate through the ionosphere
q	Production rate for the generation of electrons
L	Rate at which electrons are lost from the ionosphere (for the F_2 region the predominant loss mechanism is recombination)
\vec{v}	Motion of electrons moving in the ionosphere from all causes
\vec{F}	Force on a charged particle
\vec{B}	Magnetic field
v	Velocity of a charged particle
θ	Angle between direction of the particle velocity and the magnetic field

DEFINITION OF SYMBOLS (Cont'd)

<u>Symbol</u>	<u>Definition</u>
a	Larmor radius
v_{\perp}	component of velocity perpendicular to magnetic field lines of force
v_{\parallel}	Component of velocity parallel to magnetic field lines of force
A	Area swept out by a particle circling about a line of force
f_L	Larmor frequency
i	Current resulting from a particle in motion
E	Kinetic energy associated with the normal velocity component v_{\perp}
V_d	Drift velocity incurred by charged particles moving in a magnetic field
M	Magnetic moment

NASA-GEORGE C. MARSHALL SPACE FLIGHT CENTER

TECHNICAL MEMORANDUM X-53003

PROPOSED SOLUTION TO THE GEOMAGNETIC
ANOMALIES IN THE IONOSPHERE

By

William T. Roberts

SUMMARY

A series of graphs indicates the geomagnetic anomalies as they appear along approximately 80° W longitude. The first set depicts contours of constant frequency of f_oF_2 , the critical frequency at the F_2 peak, versus latitude, 30°S to 30°N, and local standard time, 0000 hours to 2300 hours, based on measurements at a series of IGY stations along this meridian during the months of March, July, September, and December, respectively. Since the reflected wave frequency is directly related to the square root of the electron density by the physical equation,

$$N = \frac{\epsilon_0 m \omega^2}{4\pi e^2} = 1.24 \times 10^4 f^2,$$

where N is the electron density in electrons per cm^3 , ϵ_0 is the permittivity of free space, m is the electron mass, e is the electron charge, ω is the angular frequency of the wave, and f is the "plasma resonance frequency" in Mc/sec, then, the contours may be interpreted as contours of constant electron density in order to illustrate more easily the geomagnetic anomalies. The electron density profiles exhibit both diurnal and seasonal anomalies. The primary diurnal anomaly appears as an intensification of maximum electron density at approximately 20° south and north of the geomagnetic equator between the hours of 2000 and 0000, LST. The secondary anomaly is manifested in a late morning or early afternoon reversal in the electron density gradient, $\partial N / \partial t$, at the geomagnetic equator during the spring, summer and fall months which forms a depression in the ionosphere at approximately the geomagnetic equator. A comparison of the sets of graphs shows the ionosphere to be much more active during the months of the equinoxes than during the months of the solstices. The second set shows contours of constant height of the critical frequency of the F_2 layer versus latitude and local standard time. The height of

the critical frequency of the F_2 layer exhibits an anomalous behavior at the geomagnetic equator during the early evening hours. An unusually high altitude is found to exist for the F_2 peak at approximately 1800 hours to 2000 hours, LST.

The final set of graphs depicts contours of constant electron density versus latitude and height for a typical hour for each of the months of March, July, September, and December. These graphs show an anomalous region of maximum electron density approximately twenty degrees north of the geomagnetic equator.

The article presents a solution to these anomalies based on the assumptions that (1) a geomagnetic ring current (electrojet) distorts the magnetic field lines of force at the geomagnetic equator, and (2) thermal expansion and contraction in the ionosphere produces a component of velocity, v_{\perp} , perpendicular to these lines of force.

Some measurements have already indicated the possible existence of a current stream at the assumed position; however, many more refined investigations are required in this region to determine the exact nature of the perturbing current, and to validate the remaining assumptions.

SECTION I. INTRODUCTION

For many years the ionosphere has been under investigation to determine the driving and controlling mechanisms involved. In this article the author intends to suggest a solution to the geomagnetic anomaly by assuming an interaction of two mechanisms. These two mechanisms are (1) a hypothetical geomagnetic ring current, and (2) thermal expansion and contraction of the ionosphere. By these mechanisms one may successfully explain the height and electron density profiles found in the equatorial region, within ± 30 degrees of the geomagnetic equator.

SECTION II. THE IONOSPHERE IN THEORY

In the ionosphere, electrons are produced predominantly by photo-ionization of the neutral molecules or atoms present. When electrons and ions are produced, a quantum of spectral intensity is lost. If we let $-dI$ represent this quantum of lost intensity and q represent the subsequent number of electrons produced, then

$$-dI \approx q. \quad (1)$$

The loss of intensity of spectral irradiation, $-dI$, at some height Z , in the atmosphere is in turn dependent upon the prevailing conditions at Z . The coefficient of absorption, σ , as well as the density, ρ , of the gas to be ionized must be taken into account. We also know that this spectral intensity is diminished more as it passes through a correspondingly thicker layer of atmosphere. As a result, we must consider the zenith angle, χ , of the sun. Therefore, if we have a spectral irradiation of intensity, I , incident upon a layer of gas with an increment thickness, dz , then

$$-dI = I \sigma \rho \sec \chi dz. \quad (2)$$

With the foregoing relationships firmly entrenched in our minds, we may now attempt to examine the reactions which should occur in the ionosphere and their subsequent results.

First, we assume that the earth is a sphere with a symmetrically neutral gas envelope surrounding it, and the sun is a remote lamp which turns on and off cyclically. This lamp provides certain components of illumination which are capable of photoionizing our neutral gas envelope. Now, if we examine the sphere and attempt to determine how electrons are arranged over the sphere, we should find that the maximum electron density increases as we approach the sub-solar point from any direction. We should thus expect to find, at the equinox, for instance, the maximum electron densities in the vicinity of the earth's equator at noon local standard time.

If we now attempt to measure the height of the maximum electron density, we find that even though the intensity of our radiation is penetrating deeper into the atmosphere at the sub-solar point, attempting to lower the height of maximum electron density, the atmosphere also tends to bulge at this point due to heating and counteracts this effort. Therefore, the height of the maximum electron density should reach some constant intermediate (low relative to the night height) altitude at which it remains during the day.

Now, we will allow our earth model to spin about its axis, and endeavor to determine the expected reaction along a longitudinal meridian. We will also allow the model to be illuminated by the lamp constantly.

As the sphere rotates into the light source, the electron density rapidly increases. The electron density is more predominant along the line where χ is always a minimum. At the same time, the height of maximum electron density moves closer in toward the earth, since the radiation penetrates further into the denser atmosphere.

At some time after noon, a time is reached where the production of electrons is exactly equal to the loss of electrons by their recombination. Following this the electron density gradually begins to decrease on into and through the night.

A third equation which is used to explain the ionospheric behavior is the following well known equation of continuity,

$$\frac{\partial N}{\partial t} = q - L - \text{div} (N\vec{v}), \quad (3)$$

which states that the time rate of change of electron density, N , depends upon the production of electrons, q , less the loss of electrons by (a) recombination, L , and (b) by their motions, $\text{div} (N\vec{v})$.

SECTION III. DISCUSSION OF PROBLEM

Figures 1-4 illustrate the contours of constant frequency or electron density, since they are directly dependent, of the F_2 peak as determined for a given meridian. Table I lists the stations used [2].

In general, the diurnal variation in electron density is easily explained. In the morning $\partial N / \partial t > 0$, and the contours of electron density are fairly closely spaced due to the application of irradiation, and subsequent rapid increase of electrons due to photoionization.

After about 1000 hours LST, $\partial N / \partial t$ becomes less positive with only a slight increase in electron density until approximately 1500 hours LST. It is found, however, that at the geomagnetic equator the daytime maximum electron density (N_{max}) is less than on either side.

Obviously, q will not ordinarily decrease as the zenith angle of the sun increases (since it is related to $-dI$ in equation 1), and since L is thought to be totally dependent upon N , the relatively low daytime N_{max} at the geomagnetic equator is considered to be an anomalous behavior. The divergence term is of use in accounting for the gain or loss of electrons in a region by means of their motion, and subsequently becomes very important in this region.

As evening approaches, $\partial N / \partial t < 0$, and the electron densities begin to decrease because of the loss of ionizing radiation. It is immediately noticeable that a maximum nocturnal buildup of electrons occurs north of the geomagnetic equator at approximately 2200 hours LST followed by a similar occurrence south of the equator approximately two hours later. This behavior is not at all in keeping with the continuity equation and is one of the main anomalies in the ionosphere.

The fact that the above mentioned anomaly is predominant during and around the months of equinox, and is least observable during the months of solstice, is easily explained when one considers that the ionizing radiation is proportional to $\sec \chi$ (equation 1), and at the geomagnetic equator the sun is more directly overhead in the months of the equinoxes.

Figures 5-8 are contours of height of maximum electron density $h(N_{\max})$.

After sunrise the altitude of maximum electron density becomes lower as the lower and denser atmosphere is ionized. This height remains essentially constant throughout the midday hours (from about 1000 hours to about 1500 hours). As the sun approaches the horizon, the ionizing irradiation decreases, since it must penetrate more atmosphere to reach this point. The major height anomaly occurs in the approximate location of the geomagnetic equator. An extremely high altitude for (N_{\max}) at the geomagnetic equator occurs shortly after sunset. This anomaly appears to be the most predominant in the winter, and least so in the summer. Almost immediately upon reaching a maximum the height begins to decrease, and the height anomaly disappears in about two hours.

During the remainder of the night the heights are reasonably steady from hour to hour, although they are higher than the daytime steady state.

Figures 9-12 were constructed using data obtained from the stations listed in Table II [17-19]. Essentially they represent a vertical cross section of Figures 5-8 using contours of electron density in electrons/cm³.

The main drawback of maps of this kind is that only one particular hour for one month may be illustrated per graph. In order to avoid an avalanche of graphs, only one hour of one day for each month in the northern hemisphere for the four months (March, July, September, and December) is shown.

The contours of equal electron density at once reveal that the maximum electron densities lie on the positive slope of height as one nears the geomagnetic equator from the north.

The seasonal maximum electron density continues to occur in the months of the equinox; however, the winter N_{\max} is noticeably greater than that of summer. Since the magnetic equator in this longitude lies south of the geodetic equator, one might expect the seasonal change to be less apparent in the winter.

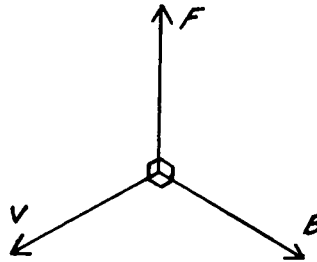
Thus, we have examined the two major parameters, N_{\max} and $h(N_{\max})$, of electron density profiles from a diurnal and a seasonal point of view.

SECTION IV. ELECTRONS IN A MAGNETIC FIELD

An electron moving in the presence of a magnetic field will undergo a force due to the magnetic field provided its motion is not parallel to the field lines of force. The magnitude of this force, F , is the familiar equation

$$F = Bev \sin \theta \quad (4)$$

where B is the magnetic field, e is the charge of the electron; v is the velocity with which the electron is moving, and θ is the angle between B and v . The force will be perpendicular to the plane made by the velocity components of the electron and the magnetic field direction at this point (Sketch 1).



Sketch 1

From elementary physics one understands that such a force as described in the preceding paragraph directs the electron in a circular orbit. The component of the velocity perpendicular to the lines of force (v_{\perp}) causes the particle to orbit with a Larmor radius (a) derived from

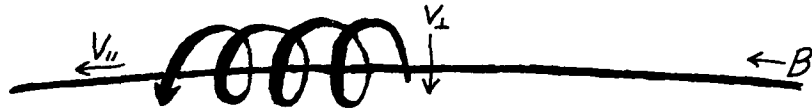
$$a = \frac{mv_{\perp}}{eB} \quad (5)$$

where m is the mass of the particle (electron). The angular velocity, or Larmor frequency (f_L) is determined by

$$f_L = \frac{v_{\perp}}{a} = \frac{eB}{m} \quad (6)$$

The component of velocity parallel to the magnetic field (v_{\parallel}) is not affected by the lines of force of the field. Therefore, v_{\parallel} will continue to act in the direction parallel to the field lines. Now, the particles are trapped by the velocity normal to the lines of force, and move with the parallel component of velocity v_{\parallel} , as in Sketch 2.

If we assume a mechanism which will perturb the existing field, as in Sketch 2, the motion of the particle naturally evolves. Since v may be rather small, the component v_{\parallel} should cause the particle to move slowly along the magnetic field lines.



Sketch 2

The spiral motion of a charged particle results in a magnetic moment whose magnitude is dependent upon the area and the current. Since the current $i = ef_L/2\pi$, and the area $A = \pi a^2$, the magnetic moment, M , is

$$M = Ai = 1/2 ef_L a^2 = 1/2 ev_{\perp} a, \quad (7)$$

or from equation (4)

$$M = 1/2 \frac{mv_{\perp}^2}{B} = \frac{E}{B} \quad (8)$$

where E is the kinetic energy of the particle normal to the magnetic field.

Assuming a relatively large flux of charged particles exist, the magnetic field may be altered to a considerable extent due to the resultant magnetic moment. If at a certain point in the upper atmosphere conditions are such that a great number of atoms are ionized, one may imagine how they may be entrapped. At the geomagnetic equator the particles could be trapped by the earth's magnetic field as they undergo vertical diffusion. Since these particles are assumed to move only up or down, then $v_{\parallel} = 0$, because B is normal to v at this point.

The particles will undergo a force, because of the dipole moment M

$$\vec{F} = (M \vec{\nabla} B) \quad (9)$$

which will result in a drift velocity

$$\vec{V}_d = \frac{1}{eB^2} (\vec{F} \times \vec{B}). \quad (10)$$

Knowing that the geomagnetic field gradient is directed toward the earth, and B is directed north, this results in a westward ring current.

SECTION V. PRESENTATION OF THEORY

Figure 1 illustrates the problem as depicted by a series of stations along a geodetic meridian. The diurnal electron density maximum is less at the magnetic equator than on either side. From equation 3, the ionospheric continuity equation,

$$\frac{dN}{dt} = q - L - \text{div} (N\vec{v}),$$

one may immediately speculate that neither q , the rate of production of electrons, nor L , the loss rate of electrons, should be markedly different at the equator than at a relatively short distance on either side. Therefore, the remaining term, $\text{div} (N\vec{v})$, must account for the anomaly.

Now assume that a ring current or electrojet is set up at the 200 to 400-km altitude over the geomagnetic equator. Further, assume that the current system is not affected by any vertical drift of the surrounding atmosphere. This places the electrojet within the ionosphere. If the normal magnetic field of the earth B_e is enhanced by the field produced by the ring current, B_i , the greater field produced may be

$$B = B_e + B_i ,$$

or using Ampere's law to calculate B_i ,

$$B = B_e + \frac{\mu_0}{4\pi} \int \frac{\vec{J} \times \hat{\gamma}^0}{\gamma^2} dV$$

where μ_0 is defined as the permeability of free space, \vec{J} is the current density carried along in the incremental volume dV , and the distance from the point being considered to the element volume dV is denoted by γ with the sense $\hat{\gamma}^0$.

In the morning, as the sun rises, the application of photon radiation to the atmosphere quickly begins to ionize the gas within this region. The expansion of the atmosphere is a slightly slower process, but when the atmosphere does begin to expand, the ions which have been formed are reluctant to enter into the regions of higher magnetic intensity set up by the ring current. Since the atmosphere must expand, the ions and electrons tend to slide around the lines of force of the ring current. As a result the regions on either side of the ring current are more heavily ionized than the equatorial region where the ring current lies.

By examining a series of contour maps, such as that of Figure 1, one immediately notices that the diurnal variation is more marked in the summer than in the winter. If one assumes that the seasonal variation may be caused by the intensity of the ring current flowing at the geomagnetic equator, and that this ring current is enhanced by the zenith angle of the sun, one may see why this difference in variation is so. If the ring current is maintained by a similar ionizing process which affects the ionosphere, it may be seen how the ring current would be enhanced through a process such as found in equation (1). That is, we might say that

$$\vec{J} \propto dI.$$

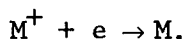
At the geographic meridian along which our stations are located, the geomagnetic equator lies considerably south of the geodetic equator. If it is further assumed that this low altitude ring current perturbs the ionosphere in general, one may logically conclude that the closer the zenith of the sun is to the geomagnetic equator the more active the ionosphere will be. It is obvious that since the geomagnetic equator lies south of the geodetic equator, the sun's zenith will be much closer to the geomagnetic equator during the winter solstice than during the

summer solstice. Further, since - at this longitude - the ring current is always in the southern hemisphere, one could expect the southern hemisphere to be less seasonably variable. The graphs substantiate this.

As evening approaches, the photon ionizing radiation diminishes since it must penetrate a much thicker layer of atmosphere. As the atmosphere contracts, the ions and electrons once again exhibit a reluctance to enter the regions of higher magnetic flux and tend to deflect north and south of the geomagnetic equator. The ions formed nearer the geomagnetic equator may be trapped within the higher magnetic field formed there. Thus, in the continuity equation the divergence term is probably small. In the evening, the production rate q is also small and so the ionosphere should be dominated primarily by the loss rate term

$$\frac{\partial N}{\partial t} \approx L.$$

In this instance, electrons are lost to the ionosphere mainly by recombination:



Since the recombination rate is proportioned to the square of the electron density, the loss rate term may be put into the form

$$L = \alpha N^2,$$

where α is the appropriate recombination coefficient.

The recombination coefficient is affected to a great extent by the proximity of an electron to a positive ion. Within the restricting region of the high magnetic field, this distance between an electron and an ion is relatively small. As a result, electrons are lost to the ionosphere rapidly within this region. One will notice that, at this time, the maximum electron content (N_{\max}) at the geomagnetic equator is very much less than in the surrounding regions (Figure 1) and occurs at a much higher altitude (Figure 5). This effect quickly dissipates as the atmosphere continues to undergo contraction, and the regions north and south of the geomagnetic equator increase in electron density due to the influx of electrons from the equatorial region. At the geomagnetic equator, the electrons rapidly descend as the atmosphere contracts. As a

result of this, the nocturnal buildup of electron density occurs on either side of the geomagnetic equator. The resulting high densities thus lag the height contours of N_{\max} at the geomagnetic equator.

SECTION VI. LIMITATIONS OF THEORY

It is at once apparent that the main objection to the theory just presented is the presence of a ring current to enhance the magnetic field at an altitude of 200 to 400 km, since we know that no ring current has actually been determined at a given altitude by satellite investigations. Nevertheless, we must not neglect the important fact that a lack of such data is not conclusive, since many experimental observations have indicated the existence of such a current.

The second question which one would probably ask concerns the lagging of the southern nocturnal buildup of electrons behind the northern. The only solution which is immediately apparent is the possibility that the rapid recombination which takes place in the northern region creates a thermal convection trend so that ions begin flowing to the southern region rather than the northern.

It would seem that many important conclusions could be drawn, if some direct measurements were made in these regions: (1) The value of T_e (the electron thermal kinetic energy) should be determined within the northern and southern regions of nocturnal buildup and compared with the normal daytime T_e ; (2) some simultaneous direct probe measurements at the geomagnetic equator would be extremely interesting; and (3) finally, we should attempt to determine the most prevalent ion in these regions at these times. The resulting data should enable us to reach a more definite solution to the geomagnetic anomalies.

TABLE I

STATIONS USED IN THE CONSTRUCTION OF FIG. 1-8
(Ref. 2)

<u>STATION</u>	<u>LATITUDE</u>	<u>LONGITUDE</u>
Bogota	4° 32' N	74° 15' W
Cape Canaveral	28° 24' N	80° 36' W
Chiclayo	6° 48' S	79° 49' W
La Paz	16° 29' S	68° 03' W
Talara	4° 34' S	81° 15' W
Puerto Rico	18° 30' N	67° 10' W
Tucuman	26° 53' S	65° 23' W
Ushuaia	54° 48' S	68° 19' W

TABLE II

STATIONS USED IN THE CONSTRUCTION OF FIG. 9-12
(Ref. 17-19)

<u>STATION</u>	<u>LATITUDE</u>	<u>LONGITUDE</u>
Washington, D. C.	38.7° N	77.0° W
Panama	9.4° N	79.9° W
Talara	4.0° S	81.5° W
Huancayo	12.0° S	75.3° W

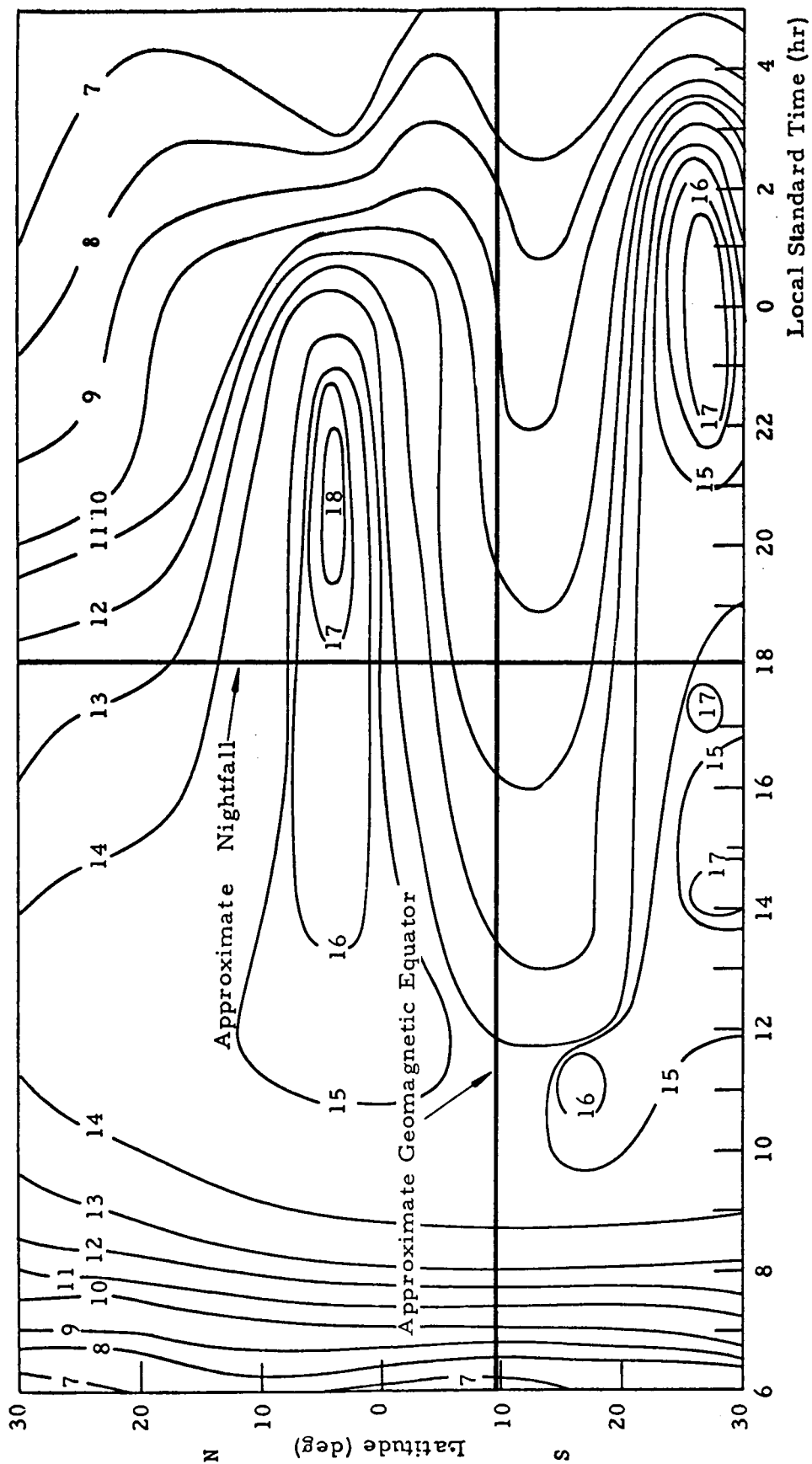


FIGURE 1. CONTOURS OF CONSTANT FREQUENCY (MC/SEC) FOR THE PEAK OF THE F₂ LAYER AVERAGED OVER THE MONTH OF MARCH 1958.

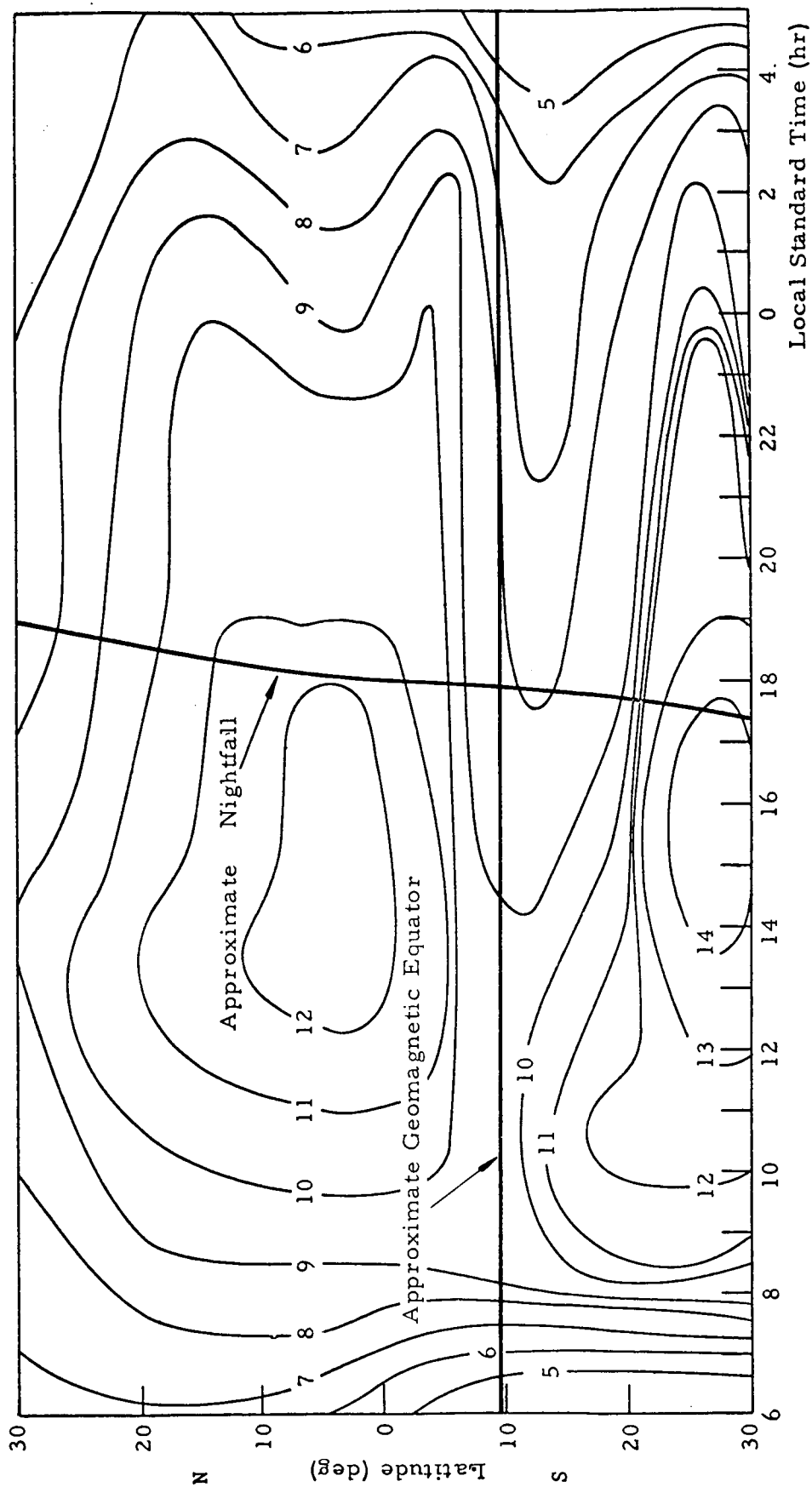


FIGURE 2. CONTOURS OF CONSTANT FREQUENCY (MC/SEC) FOR THE PEAK OF THE F₂ LAYER AVERAGED OVER THE MONTH OF JULY 1958.

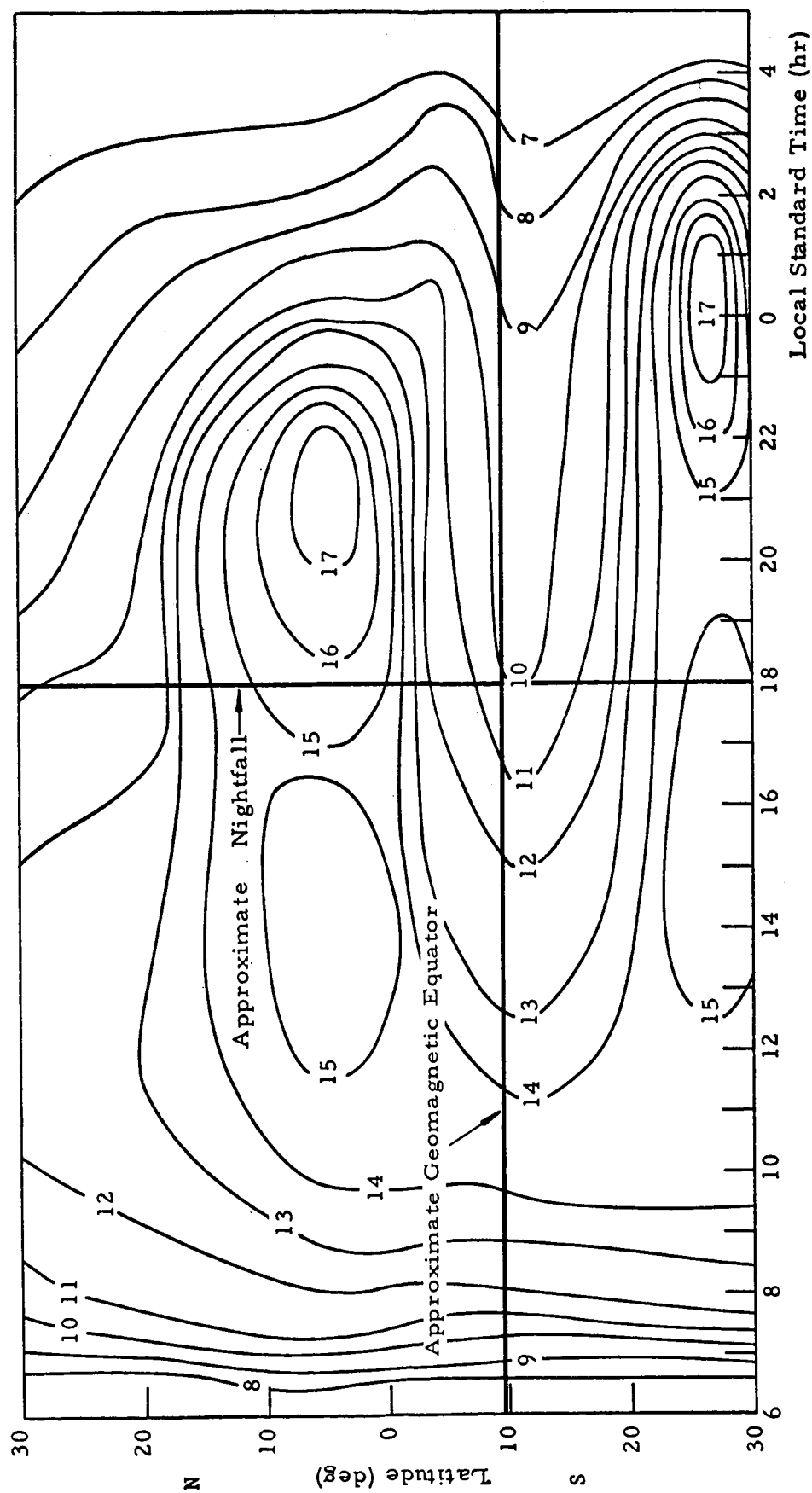


FIGURE 3. CONTOURS OF CONSTANT FREQUENCY (MC/SEC) FOR THE PEAK OF THE F_2 LAYER AVERAGED OVER THE MONTH OF SEPTEMBER 1958.

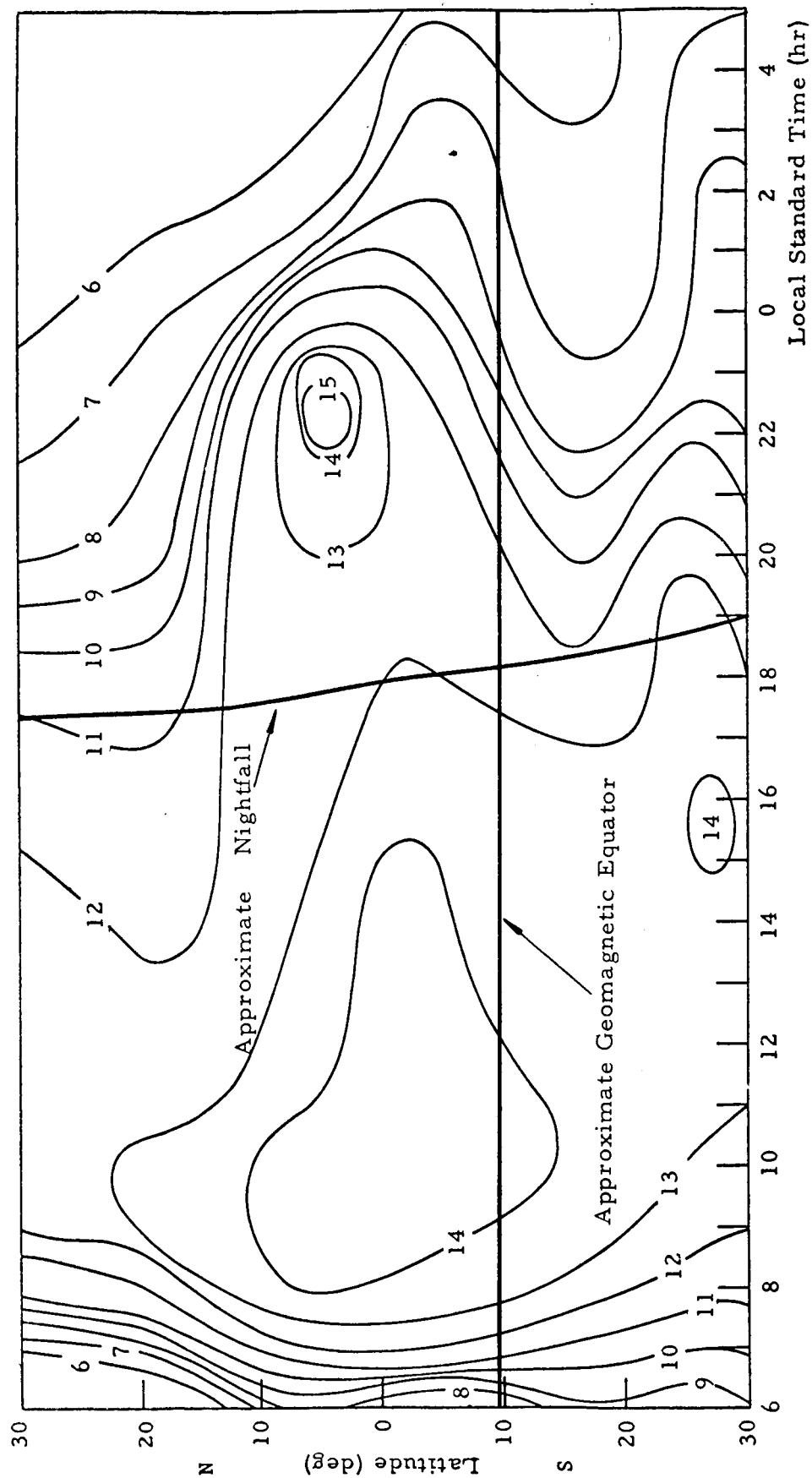


FIGURE 4. CONTOURS OF CONSTANT FREQUENCY (MC/SEC) FOR THE PEAK OF THE F_2 LAYER AVERAGED OVER THE MONTH OF DECEMBER 1958.

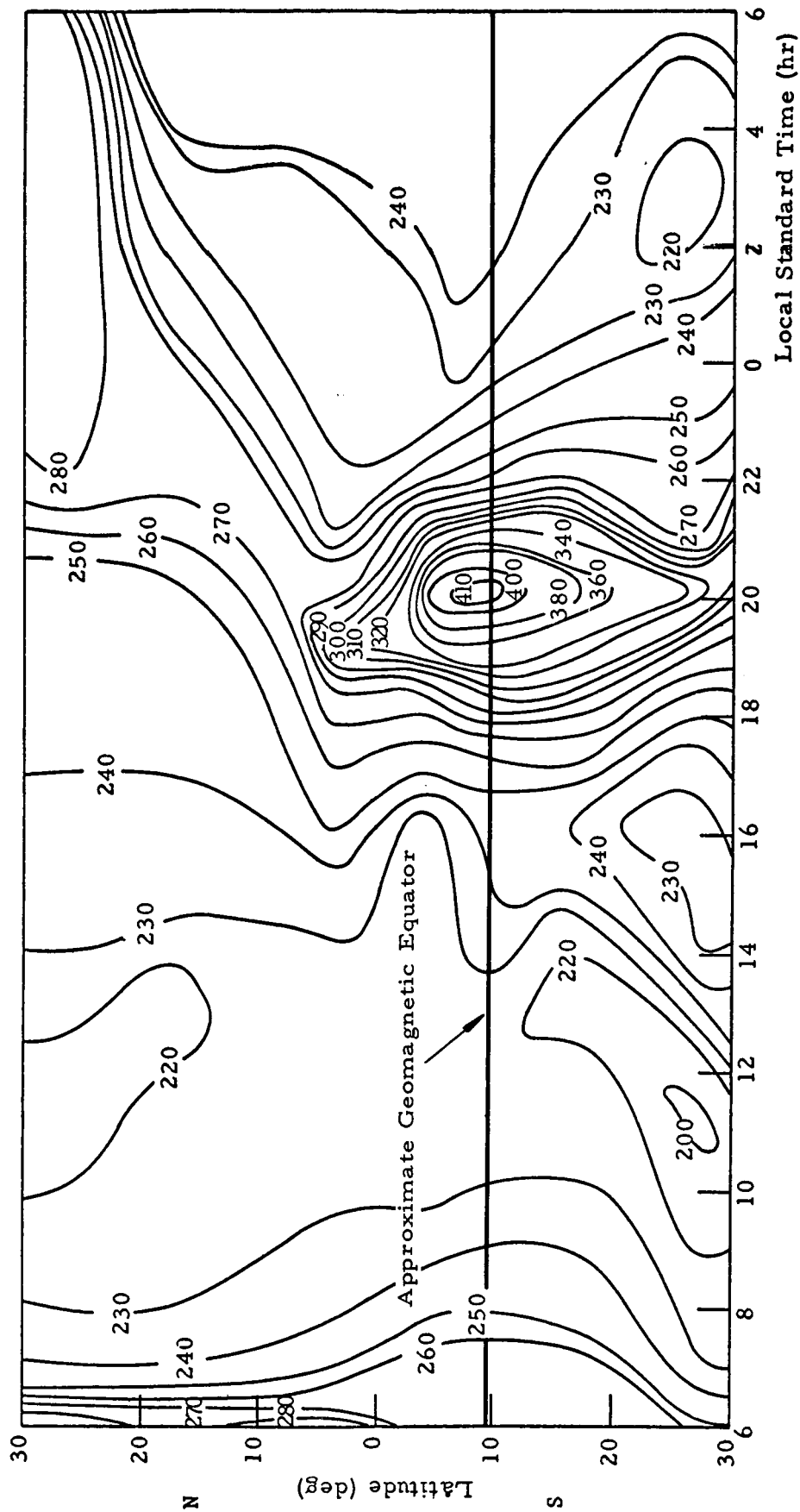


FIGURE 5. CONTOURS OF CONSTANT HEIGHT (KM) OF THE PEAK OF THE F_2 LAYER AVERAGED OVER THE MONTH OF MARCH 1958.

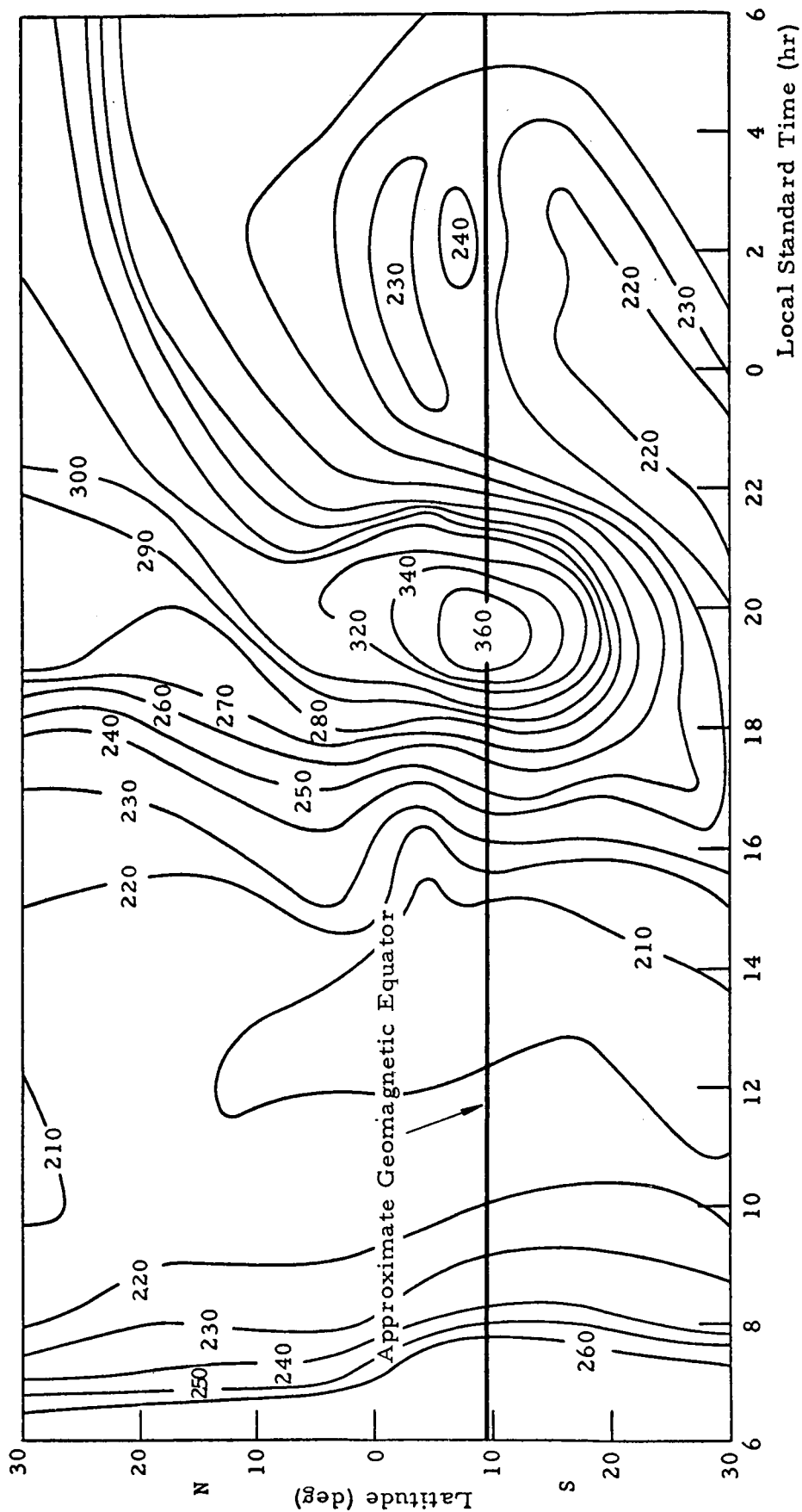


FIGURE 6. CONTOURS OF CONSTANT HEIGHT (KM) OF THE PEAK OF THE F₂ LAYER AVERAGED OVER THE MONTH OF JULY 1958.

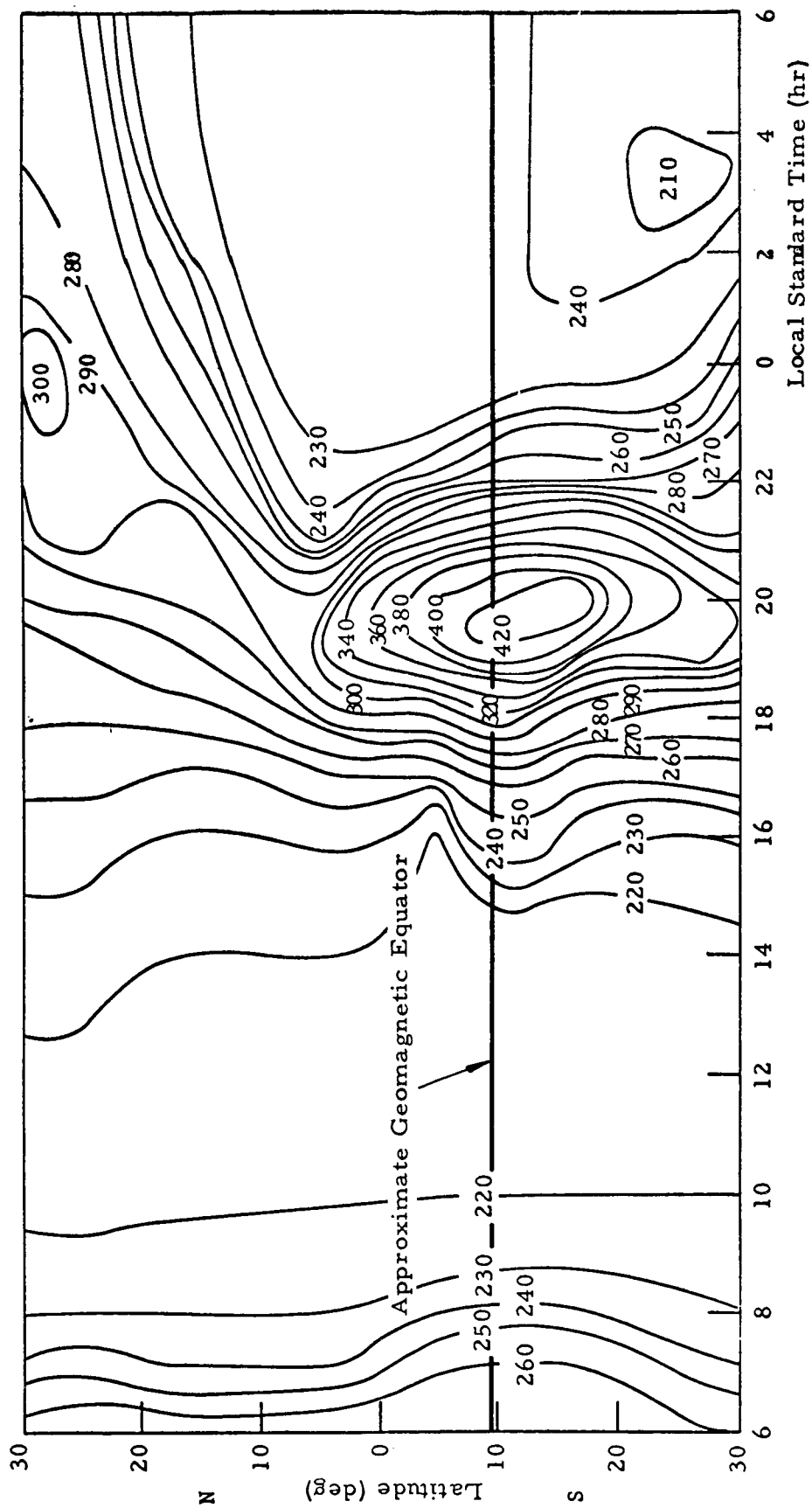


FIGURE 7. CONTOURS OF CONSTANT HEIGHT (KM) OF THE PEAK OF THE F_2 LAYER AVERAGED OVER THE MONTH OF SEPTEMBER 1958.

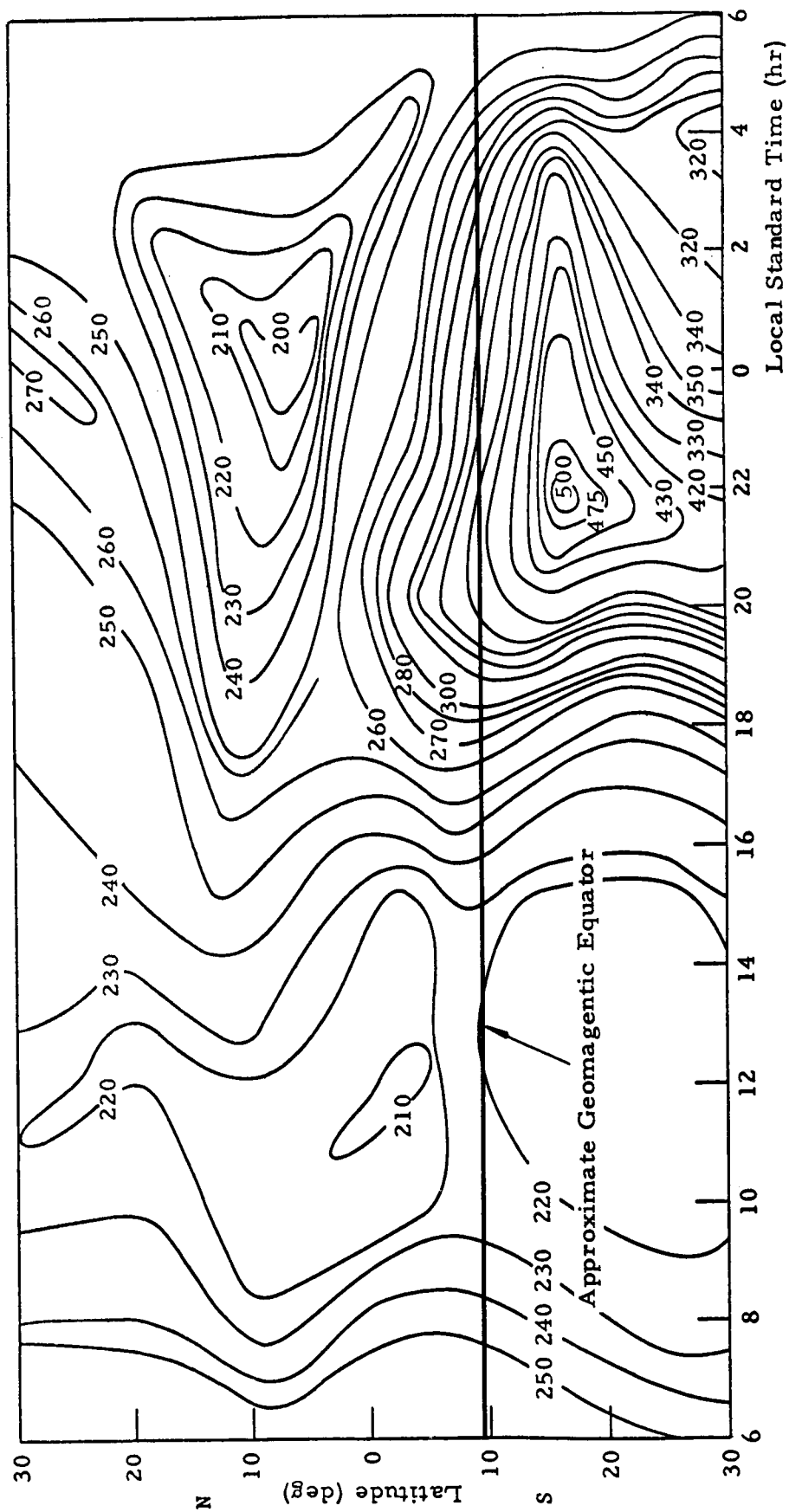


FIGURE 8. CONTOURS OF CONSTANT HEIGHT (KM) OF THE PEAK OF THE F_2 LAYER AVERAGED OVER THE MONTH OF DECEMBER 1958.

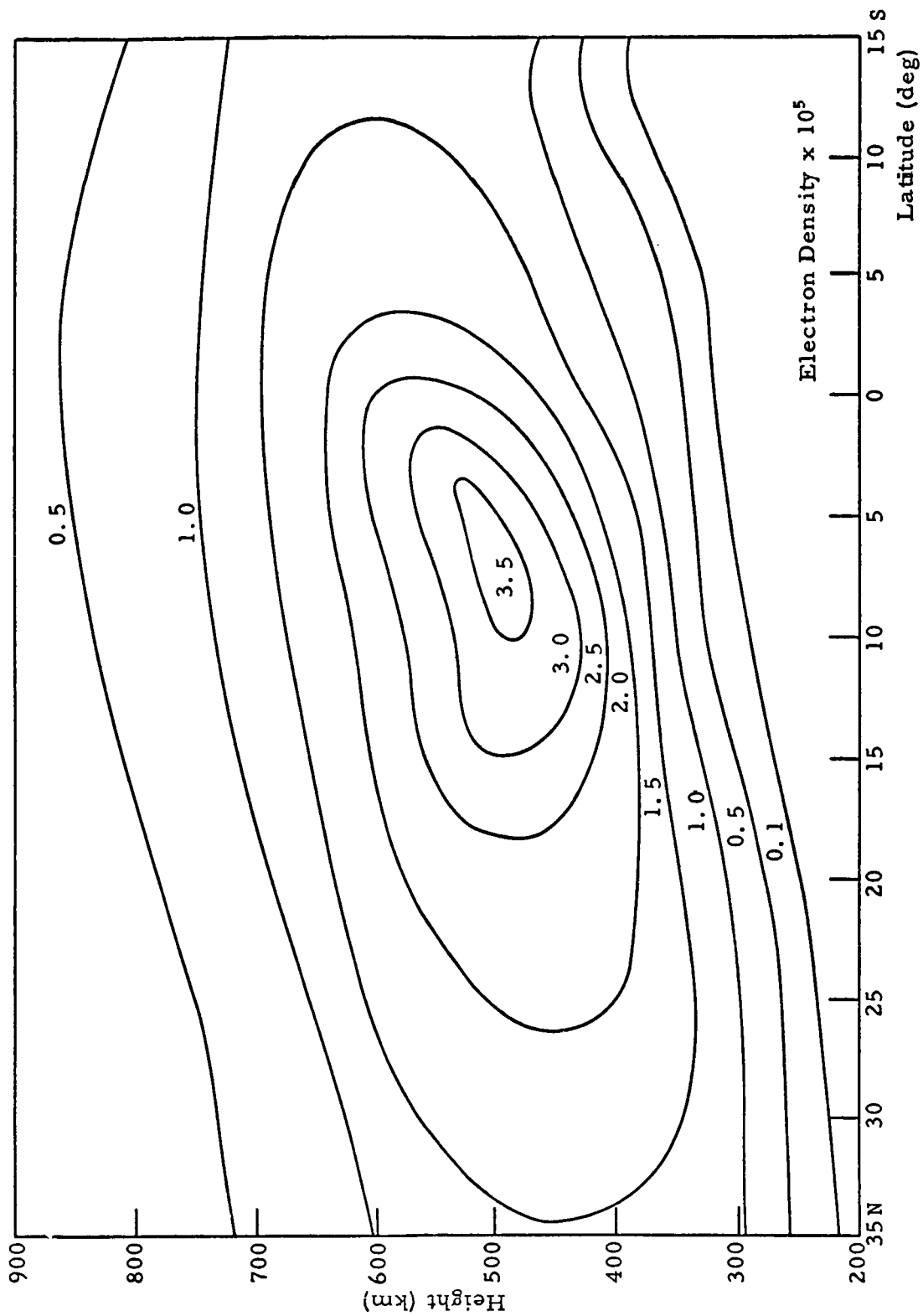


FIGURE 9. CONTOURS OF CONSTANT ELECTRON DENSITY IN ELECTRONS PER CUBIC CENTIMETER DEPICTING THE HEIGHT AND LATITUDINAL LOCATION OF THE NOCTURNAL MAXIMUM ELECTRON DENSITY AT 19:00 LST ON MARCH 21, 1958.

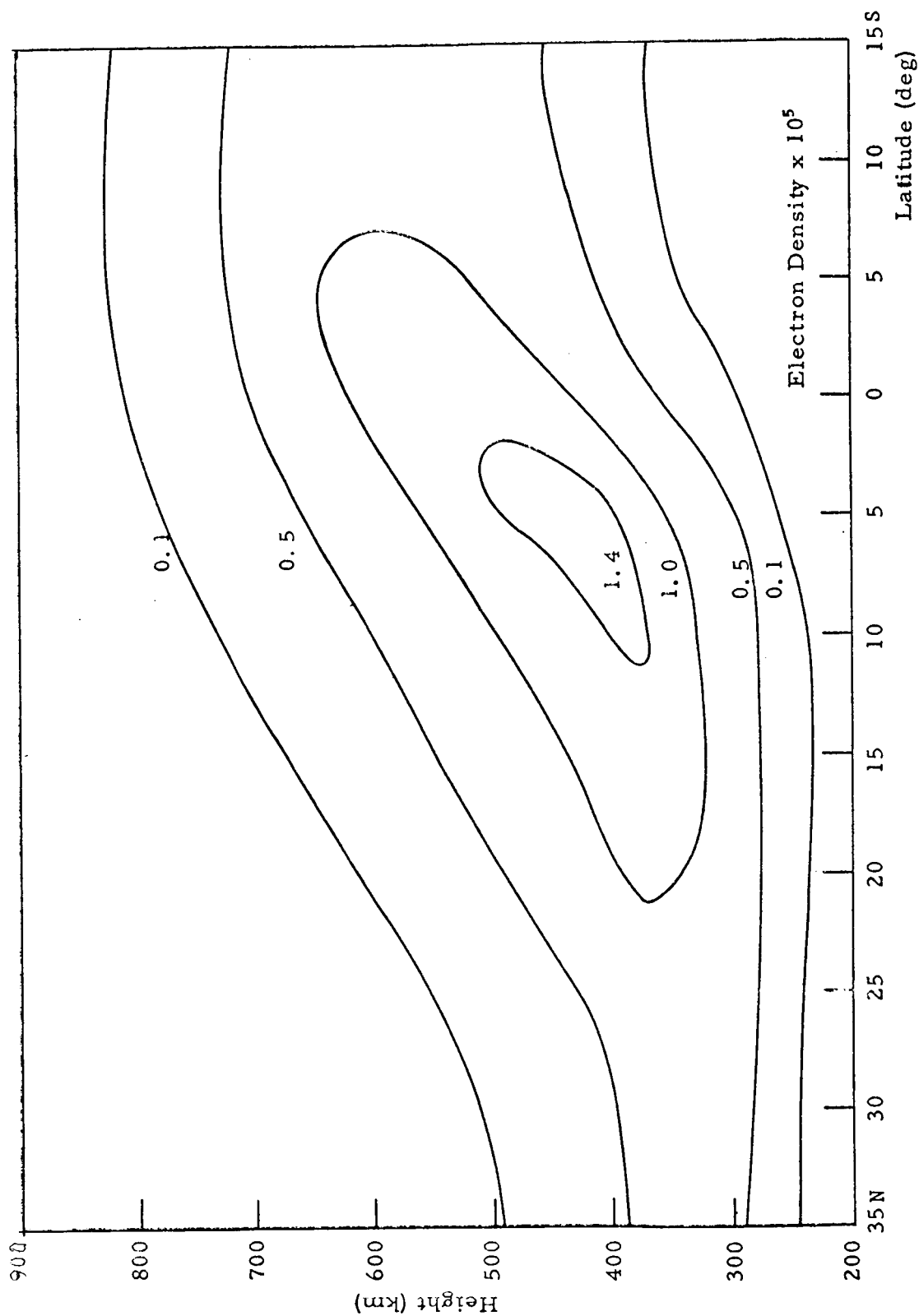


FIGURE 10. CONTOURS OF CONSTANT ELECTRON DENSITY IN ELECTRONS PER CUBIC CENTIMETER DEPICTING THE HEIGHT AND LATITUDINAL LOCATION OF THE NOCTURNAL MAXIMUM ELECTRON DENSITY AT 19:00 LST ON JULY 15, 1958.

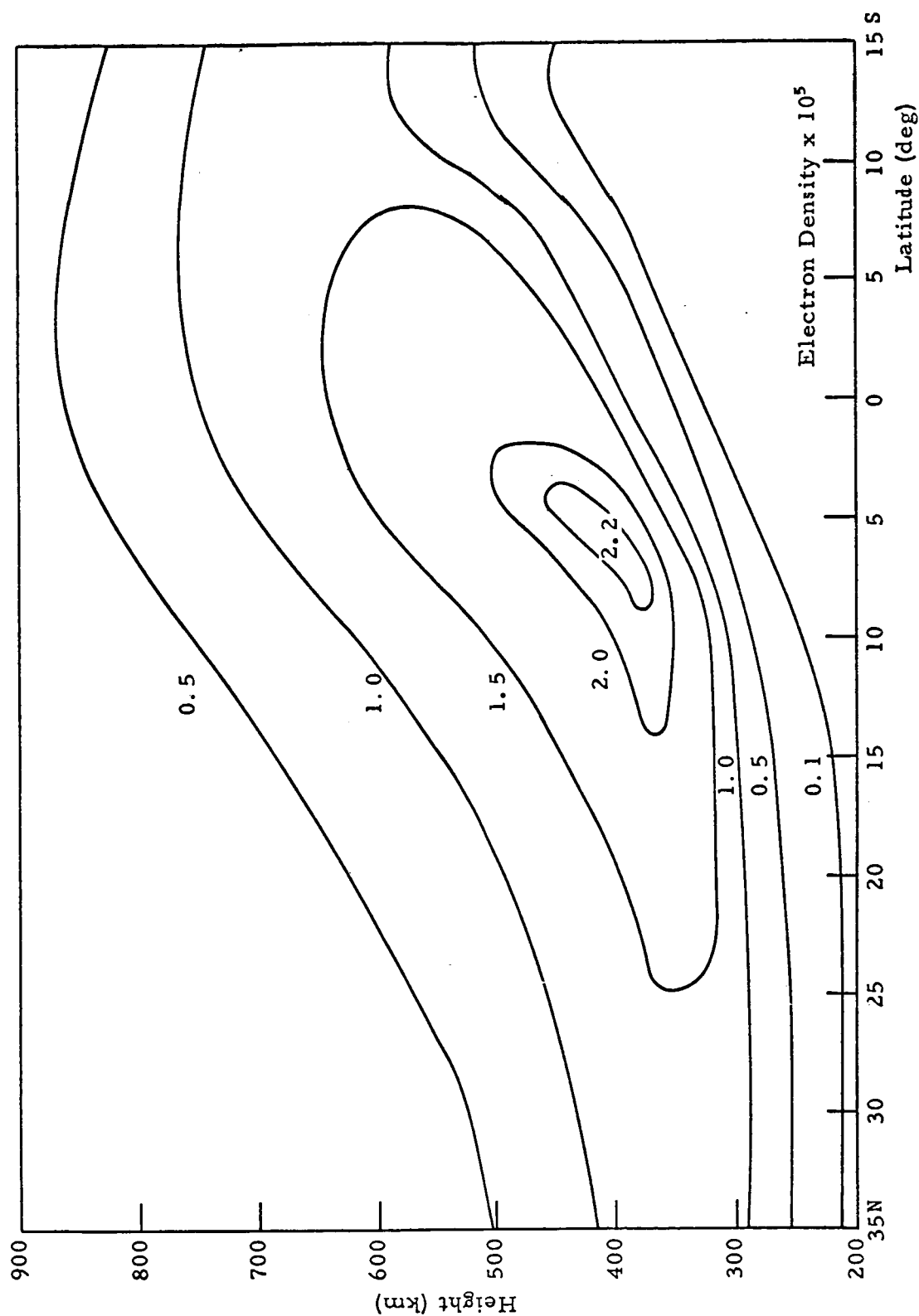


FIGURE 11. CONTOURS OF CONSTANT ELECTRON DENSITY IN ELECTRONS PER CUBIC CENTIMETER DEPICTING THE HEIGHT AND LATITUDINAL LOCATION OF THE NOCTURNAL MAXIMUM ELECTRON DENSITY AT 19:00 LST ON SEPTEMBER 22, 1958.

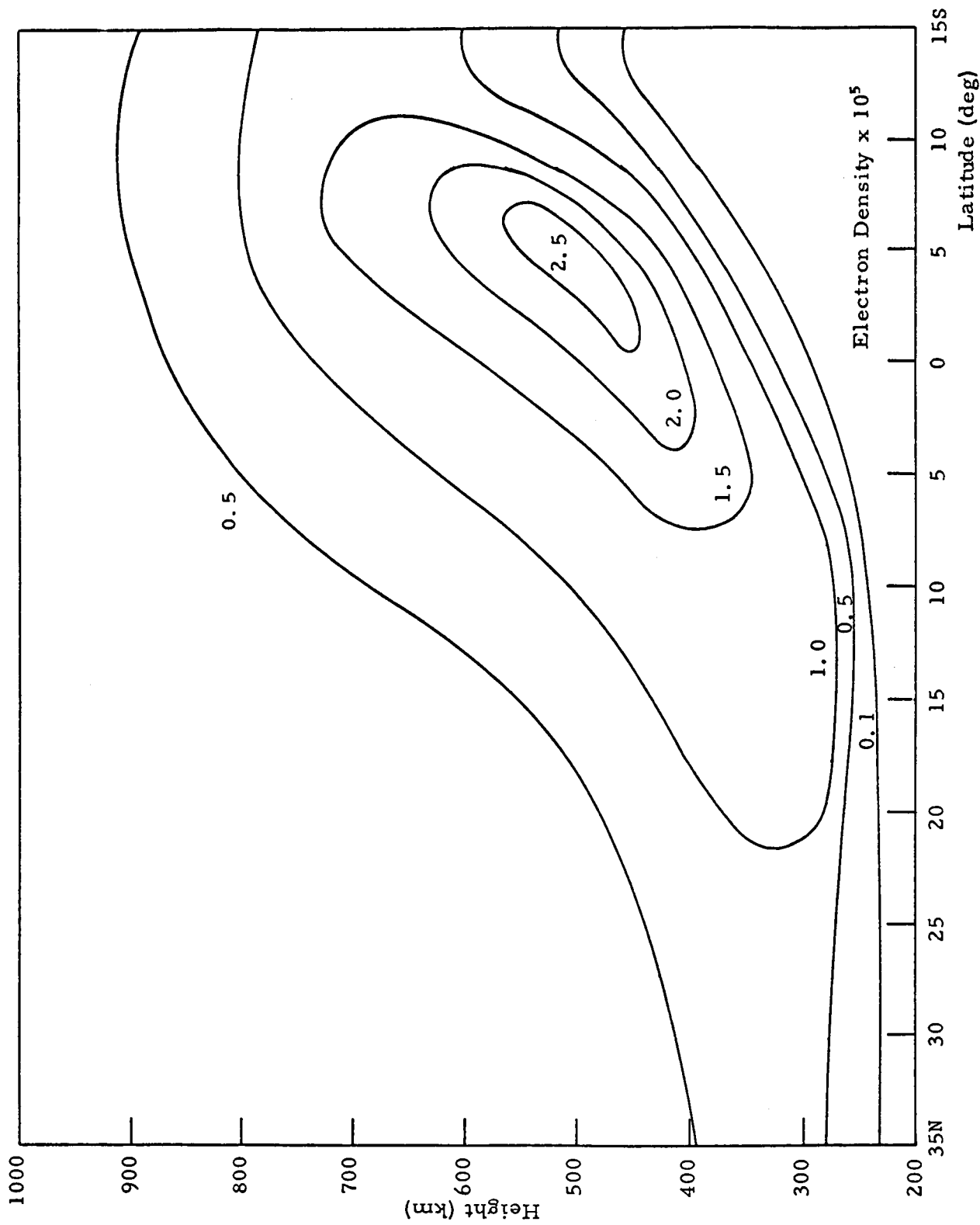


FIGURE 12. CONTOURS OF CONSTANT ELECTRON DENSITY IN ELECTRONS PER CUBIC CENTIMETER DEPICTING THE HEIGHT AND LATITUDINAL LOCATION OF THE NOCTURNAL MAXIMUM ELECTRON DENSITY AT 20:00 LST ON DECEMBER 21, 1958.

REFERENCES

1. Becker, W., "The Varying Electron Density Profile of the F-Region During Magnetically Quiet Nights," Journal of Atmospheric and Terrestrial Physics, Vol. 22, 1961, pp. 275-289.
2. Beynon, W. J. G. and C. M. Minnis, "Annals of the International Geophysical Year," Vol. XV, XVII, XVIII, and XIX, Pergamon Press, New York, 1962.
3. Blumle, L. J. and W. J. Ross, "Satellite Observation of Electron Content at the Magnetic Equator," Journal of Geophysical Research, Vol. 67, Feb. 1962, pp. 896-897.
4. Blumle, L. J., "Satellite Observations of the Equatorial Ionosphere," Journal of Geophysical Research, Vol. 67, November 1962, pp. 4601-4605.
5. Bowhill, S. A., "Rocket Measurements of F-Layer Electron Density and Their Interpretation," Journal of Atmospheric and Terrestrial Physics, Vol. 21, 1961, pp. 272-283.
6. Bowhill, S. A., "The Ionosphere," Astronautics, October 1962, pp. 80-84.
7. Bourdeau, R. E., "Ionospheric Research from Space Vehicles," NASA X-615-62-234, Greenbelt, Md., December 1962.
8. Buddin, K. G., Radio Waves in the Ionosphere, Cambridge University Press, 1961.
9. Butler, H. W., "An Investigation of Horizontal Gradients in the Electron Content of the Ionosphere," Ionosphere Research Laboratory, Pennsylvania State University, Scientific Report No. 165, July 1962.
10. Chandrasekhar, S., Plasma Physics, University of Chicago Press, 1962.
11. Chisholm, G. E., "Observations of Large Scale Ionospheric Irregularities as Deduced from Satellite Information," Pennsylvania State University, Scientific Report No. 166, August 1962.
12. Evans, J. V., "Studies of the F-Region by the Incoherent Backscatter Method," Lincoln Laboratory, Massachusetts Institute of Technology, Technical Report No. 274, July 1962.
13. Johnson, F. S., Satellite Environment Handbook, Stanford University Press, 1961.

REFERENCES (Cont'd)

14. Rastogi, R. G., "Enhancement of the Lunar Tide in the Noon Critical Frequency of the F_2 Layer over the Magnetic Equator," Journal of Research of the National Bureau of Standards, Vol. 66D, September-October 1962, pp. 601-606.
15. Ratcliff, J. A., Physics of the Upper Atmosphere, Academic Press, New York, 1960.
16. Roberts, W. T., "Properties of the F_2 Region of the Ionosphere," NASA MTP-AERO-63-23, Huntsville, Alabama, April 1963.
17. Schmerling, E. R. and D. Grant, "An Analysis of the Electron Densities in Region F of the Ionosphere," Ionosphere Research Laboratory, Pennsylvania State University, Scientific Report No. 147, April 1961.
18. Schmerling, E. R., "Ionospheric Electron Densities for Washington, D. C., Panama, Talara, and Huancayo, for October, November, and December 1958," Ionosphere Research Laboratory, Pennsylvania State University, Scientific Report No. 136, August 1960.
19. Schmerling, E. R., "Ionospheric Electron Densities for Washington, D. C., Panama, Talara, and Huancayo, for January, February, and March 1958," Ionosphere Research Laboratory, Pennsylvania State University, Scientific Report No. 122, August 1959.
20. Schmerling, E. R., "Ionospheric Electron Densities for Washington, D. C., Panama, Talara, and Huancayo, for July, August, and September 1958," Ionosphere Research Laboratory, Pennsylvania State University, Scientific Report No. 130, March 1960.
21. Seddon, J. Carl, "A Model of the Quiet Ionosphere," NASA TN D-1670, Washington, D. C., February 1963.
22. Smith, E. J., "Theoretical and Experimental Aspects of Ring Currents," Space Sciences, Jet Propulsion Laboratory, California Institute of Technology, 1963, pp. 316-374.
23. Wasko, P. E. and T. A. King, "The Earth's Aerospace Properties from 100 'to 100,000-km Altitude," NASA, MTP-AERO-63-2, Huntsville, Alabama, January 1963.
24. Wright, W. J. and L. S. Fine, "Mean Electron Density Variations of the Quiet Ionosphere," National Bureau of Standards, TN 40-2, February 1960.


REFERENCES (Cont'd)

25. Wright, J. W., "Diurnal and Seasonal Changes in Structure of the Mid-Latitude Quiet Ionosphere," Journal of Research of the National Bureau of Standards, Vol. 66D, May-June 1962, pp. 297-312.
26. Yeh, K. C. and G. W. Swenson, Jr., "Ionospheric Electron Content and Its Variations Deduced from Satellite Observations," Journal of Geophysical Research, Vol. 66, April 1961, pp. 1061-1067.

PROPOSED SOLUTION TO THE GEOMAGNETIC
ANOMALIES IN THE IONOSPHERE

William T. Roberts

The information in this report has been reviewed for security classification. Review of any information concerning Department of Defense or Atomic Energy Commission programs has been made by the MSFC Security Classification Officer. This report, in its entirety, has been determined to be unclassified. This report also has been reviewed and approved for technical accuracy.



William T. Roberts
Aerospace Technologist



Robert E. Smith
Chief, Space Environment Branch



William W. Vaughan
Chief, Aero-Astrophysics Office



E. D. Geissler
Director, Aero-Astrodynamic Lab.

DISTRIBUTION

TM X-53003

INTERNAL

DEP-A
R-FP-DIR
R-SP-DIR

DIR
MS-H
CC-P
HME-P

R-ASTR

Director
Mr. F. Digesu
Mr. J. Boehm

R-COMP

Director
Mr. David Aichele

R-RP

Director
Mr. G. Heller
Dr. W. Johnson
Dr. E. A. Mechtly
Dr. R. Shelton
Mr. A. Thompson

R-AERO

Dr. E. D. Geissler	-DIR
Mr. O. C. Jean	-DIR
Dr. R. F. Hoelker	-G
Mr. P. J. deFries	-S
Mr. W. K. Dahm	-A
Mr. H. J. Horn	-D
Mr. O. C. Holderer	-A
Dr. F. Speer	-F
Mr. H. F. Kurtz	-FO
Mr. W. Murphree	-T
Dr. W. Hyebe	-T
Dr. H. Sperling	-T
Mr. W. W. Vaughan	-Y
Mr. C. Dalton	-Y
Mr. J. Scoggins	-Y
Mr. O. Smith	-YT
Mr. R. Smith	-YS
Mr. H. Euler	-YS
Mr. W. Roberts (25)	-YS

R-DIR, Mr. Weidner

MS-IP
MS-IPL (8)

DISTRIBUTION (Cont'd)

EXTERNAL

NASA
Manned Spacecraft Center
Houston 1, Texas
Attn: Director
Chief, Space Environment Division
Technical Library

NASA
Lewis Research Center
21000 Brookpark Road
Cleveland 35, Ohio
Attn: Technical Library

NASA
Ames Research Center
Moffett Field, California
Attn: Technical Library

NASA
Goddard Space Flight Center
Greenbelt, Maryland
Attn: Mr. R. E. Boundeau
Planetary Ionospheres Branch
Space Sciences Division
Technical Library

NASA
Langley Research Center
Langley Station
Hampton, Virginia
Attn: Mr. Edward W. Leyhe
Technical Library

NASA
Launch Operations Center
Cocoa Beach, Florida
Attn: Director
Dr. H. Knothe
Dr. R. Bruns

DISTRIBUTION (Cont'd)

EXTERNAL (Cont'd)

NASA
Jet Propulsion Laboratory
4800 Oak Grove Drive
Pasadena, California
Attn: Dr. Conway Synder

Air Force Cambridge Research Laboratories
L. G. Hanscom Field
Bedford, Massachusetts
Attn: Technical Library

Mr. Peter E. Wasko, A2-260
Physics/Thermodynamics Section
Missile & Space Systems Division
Douglas Aircraft Company, Inc.
Santa Monica, California

Scientific and Technical Information Facility (25)
Attn: NASA Representative (S-AK/RKT)
P. O. Box 5700
Bethesda, Maryland

Mr. J. M. Boyer
Northrop Space Laboratories
Hawthorne, California

Dr. J. W. Wright
Ionosphere Research & Propagation Division
National Bureau of Standards
Boulder, Colorado

NASA Headquarters
Office of Space Sciences
Washington 25, D. C.
Attn: Dr. H. Newell, Director (2)